Published in final edited form as:
Nat Neurosci. 2016 April ; 19(4): 554–556. doi:10.1038/nn.4266.

Biophysical constraints of optogenetic inhibition at presynaptic terminals

Mathias Mahn[1], **Matthias Prigge**[1], **Shiri Ron**[1], **Rivka Levy**[1], and **Ofer Yizhar**[1]
[1]Department of Neurobiology, Weizmann Institute of Science, Rehovot 76100, Israel

Abstract

We investigated the efficacy of optogenetic inhibition at presynaptic terminals using halorhodopsin, archaerhodopsin and chloride-conducting channelrhodopsins. Precisely timed activation of both archaerhodopsin and halorhodpsin at presynaptic terminals attenuated evoked release. However, sustained archaerhodopsin activation was paradoxically associated with increased spontaneous release. Activation of chloride-conducting channelrhodopsins triggered neurotransmitter release upon light onset. Our results indicate that the biophysical properties of presynaptic terminals dictate unique boundary conditions for optogenetic manipulation.

Testing whether a particular projection pathway is involved in a defined behavioral or physiological process often requires prolonged inhibition of specific axonal projections during behavioral trials or electrophysiological recordings. The hyperpolarizing effects of light-gated chloride pumps1, 2, proton pumps3 and chloride channels4–6 on action potential firing in neuronal somata have been widely characterized2–6. Although light-driven ion pumps attenuate synaptic transmission when activated in presynaptic terminals7–9, the direct effects of these tools on presynaptic terminal function have not been characterized in detail. We therefore asked whether inhibitory optogenetic tools can be used to achieve sustained, efficient silencing of neurotransmitter release from presynaptic terminals of long-range axonal projections.

We first investigated the effects of the most widely-used inhibitory optogenetic tools, archaerhodopsin and halorhodopsin, on the activity of presynaptic terminals. To record presynaptic terminal activity, we co-expressed a synaptophysin-GCaMP6s fusion protein (SyGCaMP6s) with the membrane trafficking-enhanced archaerhodopsin or halorhodopsin variants of these opsins (eArch3.0-mCherry3, 10 or eNpHR3.0-mCherry1, 10, respectively) in cultured rat hippocampal neurons. The fluorescence labeling of SyGCaMP6s co-localized

Correspondence should be addressed to O.Y. (ofer.yizhar@weizmann.ac.il): Ofer Yizhar, Ph.D., Department of Neurobiology, Weizmann Institute of Science, 234 Herzl st., Rehovot, 76100, Israel.

Contributions
M.M. and O.Y. designed the study. M.M. performed all electrophysiology and imaging experiments. R.L. prepared neuronal cultures and viral vectors. M.P. and S.R. helped with cloning and viral injections. M.M. and O.Y. analyzed and interpreted the results and wrote the manuscript.

Competing financial interests
The authors declare no competing financial interests.

Europe PMC Funders Author Manuscripts

with the endogenous presynaptic protein synapsin I (Fig. 1a), confirming its presynaptic localization11, and mCherry fluorescence was observed both in soma and neurite membranes (Supplementary Fig. 1). Two-photon calcium imaging of spontaneous activity in these neurons showed a pattern of regularly occurring network bursts and individual bouton calcium dynamics (Supplementary Video 1). We reasoned that optogenetic inhibition would reduce the amplitude and/or frequency of presynaptic calcium transients measured by SyGCaMP6s. Surprisingly, a 5-minute–long activation of eArch3.0 caused a significant increase in SyGCaMP6s fluorescence that recovered only partially following the termination of yellow light illumination (Fig. 1b–d and Supplementary Video 2). Neurons expressing a cytoplasmic GCaMP6s also showed increased somatic and dendritic fluorescence upon eArch3.0 activation (Supplementary Video 3). In contrast, neurons expressing SyGCaMP6s alone or with eNpHR3.0-mCherry showed no detectable change in fluorescence upon illumination (Fig. 1c,d and Supplementary Videos 1 and 4). Maximal SyGCaMP6s fluorescence during eArch3.0 activation was 16.47 ± 3.84 fold (mean ± s.e.m) higher than the maximal fluorescence recorded during the baseline period (Fig. 1e).

To examine whether the eArch3.0-induced increase in presynaptic $[Ca^{2+}]_i$ leads to increased neurotransmitter release, we recorded from hippocampal neurons expressing eArch3.0 and SyGCaMP6s (Fig. 1f–h). Activation of eArch3.0 as described above led to a gradual three-fold rise in the rate of excitatory post-synaptic currents (EPSCs; Fig. 1f,g). Both eNpHR3.0-expressing and control neurons showed no change from baseline during illumination, consistent with the calcium imaging data (Fig. 1f–h). These findings indicate that eArch3.0 activation leads to a paradoxical increase in presynaptic $[Ca^{2+}]_i$ and neurotransmitter release.

We next tested whether activation of proton or chloride pumps in presynaptic terminals effectively inhibits action potential-evoked neurotransmitter release. We injected adult mice with AAVs co-expressing eArch3.0 or eNpHR3.0 with SyGCaMP6s into the whisking thalamus, which projects to the S1 barrel cortex. In acute coronal slices, we observed mCherry-labeled thalamocortical projections terminating in S1 (Fig. 2a). Electrical microstimulation of these thalamocortical fibers in the external capsule evoked reliable excitatory and inhibitory post-synaptic currents (eEPSCs and eIPSCs) in layer 4 (S1 L4) neurons (Fig. 2b; Supplementary Fig. 2a), which were attenuated by activation of both eArch3.0 and eNpHR3.0 with 200 ms light pulses (Fig. 2c,f; Supplementary Fig. 2c,g), leading to an increase in the paired-pulse ratio (Fig. 2d,g; Supplementary Fig. 2d,h). Notably, in both eArch3.0- and eNpHR3.0-expressing slices we observed strong rebound-like synaptic responses after light offset that were attenuated when step-like termination of light was replaced by a more gradual decrease in light power (Supplementary Fig. 3). These results indicate that brief illumination of axonal terminals expressing eArch3.0 or eNpHR3.0 can attenuate synaptic transmission, but is associated with strong rebound responses that can be avoided by ramp-like light termination.

To evaluate the potential of eArch3.0 and eNpHR3.0 for sustained inhibition of synaptic transmission, we recorded responses of S1 L4 neurons to microstimulation of thalamocortical fibers during 5 min of constant illumination (Fig. 2e,h). Microstimulation-evoked EPSCs and IPSCs in L4 neurons were attenuated during 5 min of eArch3.0 activation (Fig. 2e and Supplementary Fig. 2e). Inhibition of presynaptic release by

eNpHR3.0 was maximal within 50 ms of light onset and its efficacy – although still significant – was reduced approximately 2-fold after 150 ms (Fig. 2h , Supplementary Fig. 2i, Supplementary Fig. 4), likely contributing to the increase in paired pulse ratio observed with eNpHR3.0 (Fig. 2g).

We next asked whether presynaptic $[Ca^{2+}]_i$ and spontaneous release are affected in the acute slice preparation by optogenetic hyperpolarizing tools in a manner similar to that observed in our cultured neuron recordings. Presynaptic SyGCaMP6s fluorescence in thalamocortical boutons increased during activation of eArch3.0, but not eNpHR3.0 (Fig. 2i,j). Consistently, the rate of spontaneous EPSCs and IPSCs increased during activation of eArch3.0, but not eNpHR3.0, in thalamocortical terminals (Fig. 2k-n). These results indicate that activation of eArch3.0 induces a significant increase in presynaptic $[Ca^{2+}]_i$ and in spontaneous neurotransmitter release. Since thalamocortical projections are glutamatergic, the increase in spontaneous IPSCs indicates that local-circuit feed-forward inhibition12, 13 might be recruited by this rise in spontaneous excitatory input (Supplementary Fig. 6d).

For a more detailed understanding of the paradoxical effects of eArch3.0 on presynaptic function, we first tested whether the light-evoked increase in SyGCaMP6s signal is due to influx of extracellular Ca^{2+}. Removal of extracellular Ca^{2+} strongly attenuated the light-induced elevation in SyGCaMP6s fluorescence (Fig. 3a–c) and eliminated the increase in EPSC rates (Fig. 3d,e). The light-induced increase in the SyGCaMP6s signal or EPSC rates was not action potential-dependent (Fig. 3f–i). In cultured neurons, eArch3.0 photocurrents strongly adapted during 5 min of light application and this adaptation was greatly reduced by intracellular pH stabilization via addition of L-lactate to the recording medium (Supplementary Fig. 5). This led us to hypothesize that intracellular alkalization contributes to eArch3.0 effects on synaptic function. Indeed, pH-sensitive dye imaging showed that eArch3.0 activation led to an increase in intracellular pH, which was attenuated by inclusion of L-lactate in the recording medium (Supplementary Fig. 6a–c). eArch3.0-expressing cells recorded in L-lactate medium displayed attenuated Ca^{2+} influx (Fig. 3f,g) and reduced EPSC rates during illumination (Fig. 3h,i). These findings are consistent with previous work showing that intracellular alkalization triggers calcium influx in neurons14, 15 (Supplementary Fig. 6d).

Finally, we tested whether light-gated chloride channels6 can inhibit synaptic transmission via shunting of action potential-mediated release. In cultured hippocampal neurons expressing GtACR16, light-gated photocurrents allowed robust inhibition of action potential firing (Supplementary Fig. 7a,b). We next expressed GtACR1 in the whisking thalamus and recorded from S1 L4 neurons as described above. Illumination of GtACR1-expressing presynaptic terminals evoked strong, short-latency EPSCs that were similar in amplitude to the post-synaptic responses evoked by microstimulation of thalamocortical inputs to the same cells (Supplementary Fig. 7c,d). When light and microstimulation were co-applied with varying delays, light administration did not attenuate microstimulation-evoked EPSCs (Supplementary Fig. 7e,f). Increased expression levels or improved axonal targeting of these channels may provide more efficient shunting of synaptic release but would most likely not eliminate the light onset-associated responses.

Our findings uncover the biophysical constraints of optogenetic inhibition at presynaptic terminals. We show that while light-gated proton and chloride pumps can effectively attenuate neurotransmission, sustained proton pump activity in synaptic terminals induces a pH-dependent calcium influx that leads to increased spontaneous release at the target circuit. Consistent with previous reports of a depolarized chloride reversal potential in presynaptic terminals16–18, we found that activation of light-gated chloride channels triggers neurotransmitter release upon light onset, potentially limiting the utility of these tools for temporally precise manipulation of synaptic release. Our data therefore suggest that eNpHR3.0 is currently the most suitable tool for synaptic terminal silencing, although its use should be carefully controlled to account for changes in chloride reversal potential19 and strong light-off rebound responses. We expect that further optimization of light-gated potassium channels20 will allow improvements in the efficacy of fast optogenetic inhibition of neurotransmitter release.

Online Methods

Cloning of SyGCaMP6s expression vectors

GCaMP6s21 was fused in-frame to synaptophysin22 and ligated into the Cre-dependent pAAV-hSyn-DIO-WPRE backbone23. A Cre-independent version of this expression plasmid was generated by treatment of the DIO vector with Cre recombinase (NEB) *in vitro.*

Production of recombinant AAV vectors

HEK293 cells were seeded at 25%-35% confluence. The cells were transfected 24 h later with plasmids encoding AAV rep, cap and a vector plasmid for the rAAV cassette expressing the relevant DNA using the PEI method24. Cells and medium were harvested 72 h after transfection, pelleted by centrifugation (300 g), resuspended in lysis solution ([mM]: 150 NaCl, 50 Tris-HCl; pH 8.5 with NaOH) and lysed by three freeze-thaw cycles. The crude lysate was treated with 250 U benzonase (Sigma) per 1 ml of lysate at 37°C for 1.5 h to degrade genomic and unpackaged AAV DNA before centrifugation at 3000 g for 15 min to pellet cell debris. The virus particles in the supernatant (crude virus) were purified using heparin-agarose columns, eluted with soluble heparin, washed with phosphate buffered saline (PBS) and concentrated by Amicon columns. Viral suspension was aliquoted and stored at –80°C. Viral titers were measured using real-time PCR. AAV vectors used for intracranial injections had genomic titers ranging between 1.49×10^{11} and 3.28×10^{11} genome copies per milliliter (gc/ml). AAV vectors used for neuronal culture transduction had titers ranging between 1.08×10^{10} and 3.15×10^{10} gc/ml.

Primary hippocampal neuron culture and viral transduction

Primary cultured hippocampal neurons were prepared from male and female P0 Sprague-Dawley rat pups (Envigo). CA1 and CA3 were isolated, digested with 0.4 mg ml^{-1} papain (Worthington), and plated onto glass coverslips pre-coated with 1:30 Matrigel (Corning). Cultured neurons were maintained in a 5% CO_2 humidified incubator with Neurobasal-A medium (Invitrogen) containing 1.25% fetal bovine serum (FBS, Biological Industries), 4% B-27 supplement (Gibco), 2 mM Glutamax (Gibco) and plated on coverslips in a 24-well plate at a density of 65,000 cells per well. To inhibit glial overgrowth, 2 mg ml^{-1}

fluorodeoxyuridine (FUDR, Sigma) was added after 4 days of *in vitro* culture (DIV). One µl viral suspension of SyGCAMP6s (AAV2/1.hSyn1.SyGCaMP6s.WPRE) alone or mixed with 1 µl eArch3.0 (AAV2/1.CamKIIα.eArch3.0-mCherry.WPRE) or 3 µl eNpHR3.0 (AAV2/1.CamKIIα.eNpHR3.0-mCherry.WPRE) was added after 5 DIV. GtACR1 was expressed by transducing the neuronal cultures with 1 µl of AAV2/1.hSyn.GtACR1.eGFP. Cultured neurons were used between 12 – 17 DIV for experiments.

Immunohistochemistry

Hippocampal neuronal cultures were fixed for 15 min with 4% paraformaldehyde in PBS 1 week after virus transduction. Coverslips were washed three times in PBS, incubated in blocking solution for 45 min (10% normal donkey serum (NDS) with 0.1% Triton in PBS) and then exposed over night at 4°C to polyclonal rabbit anti-Synapsin I primary antibody11 (diluted 1:1000 in 5% NDS, PBS; catalog #51-5200; Invitrogen). Following 3 washes in PBS, coverslips were incubated for 2 h at room temperature (RT) with a donkey anti-rabbit Cy5-or Alexa488-conjugated secondary antibody (diluted 1:500 in 5% NDS, PBS; 711-175-152; Jackson ImmunoResearch Laboratories and A-21206; Thermo Fisher Scientific), and then washed 2 times with PBS, dipped briefly into double-distilled water and mounted on glass slides using DABCO mounting medium. Immunostained neurons were imaged with a confocal scanning microscope (LSM 700, Zeiss) using an oil immersion objective (63x, NA 1.40; Zeiss). SyGCaMP6s and Cy5 fluorescence was excited using 488 nm and 639 nm laser diodes, respectively. Alexa488 and mCherry fluorescence was excited using 488 nm and 555 nm laser diodes, respectively.

Stereotactic injection of viral vectors for acute brain slice experiments

Six-week-old female C57BL/6 mice (P35–45) were initially induced with ketamine (80 mg/kg) and xylazine (10 mg/kg) before isoflurane anesthesia (˜1% in O_2, v/v). To achieve viral expression in the thalamocortical axons from the ventral posterior medial (VPM) and posterior medial (PoM) thalamic nuclei (the main thalamic inputs to the S1 barrel cortex), a small hole (˜1 × 1 mm) was made over the ventral posteromedial thalamic nucleus (1.82 mm posterior and 1.5 mm lateral to bregma). Purified rAAV2/1 particles encoding the presynaptic Ca^{2+} indicator SyGCaMP6s (AAV2/1.hSyn1.SyGCaMP6s.WPRE) were mixed with rAAV2/1 particles encoding either the proton pump eArch3.0 (AAV2/1.CamKIIα.eArch3.0-mCherry.WPRE) or the chloride pump eNpHR3.0 (AAV2/1.CamKIIα.eNpHR3.0-mCherry.WPRE). AAV particles encoding the chloride channel GtACR1 (AAV2/1.hSyn.GtACR1-eGFP) were used unmixed. Virus suspensions were slowly injected (1 µl at 100 nl min^{-1}) using a 34 G beveled needle at a depth of 4 mm from bregma. The incision was closed with tissue glue and 0.05 mg/kg Buprenorphine was intraperitoneally injected for post-surgical analgesia. Up to 5 mice were housed in a 12 h light 12 h dark cycle for 6-10 weeks to allow for virus expression before acute brain slices were prepared. All experimental procedures were approved by the Institutional Animal Care and Use Committee (IACUC) at the Weizmann Institute of Science.

Acute brain slice preparation

Mice were injected intraperitoneally with pentobarbital (130 mg/kg, i.p.) and perfused with carbogenated (95% O_2, 5% CO_2) ice-cold slicing solution ([mM] 2.5 KCl, 11 glucose, 234

sucrose, 26 $NaHCO_3$, 1.25 NaH_2PO_4, 10 $MgSO_4$, 2 $CaCl_2$; 340 mOsm). After decapitation, 300 μm coronal barrel cortex slices were prepared in carbogenated ice-cold slicing solution using a vibratome (Leica VT 1200S) and allowed to recover for 20 min at 33°C in carbogenated high-osmolarity artificial cerebrospinal fluid (high-Osm ACSF; [mM] 3.2 KCl, 11.8 glucose, 132 NaCl, 27.9 $NaHCO_3$, 1.34 NaH_2PO_4, 1.07 $MgCl_2$, 2.14 $CaCl_2$; 320 mOsm) followed by 40 min incubation at 33°C in carbogenated ACSF ([mM] 3 KCl, 11 glucose, 123 NaCl, 26 $NaHCO_3$, 1.25 NaH_2PO_4, 1 $MgCl_2$, 2 $CaCl_2$; 300 mOsm). Subsequently, slices were kept at RT in carbogenated ACSF until use. The recording chamber was perfused with carbogenated ACSF at a rate of 2 ml min^{-1} and maintained at 32°C.

Electrophysiological methods

Whole-cell patch clamp recordings were performed under visual control using oblique illumination on a two-photon laser scanning microscope (Ultima IV, Bruker) equipped with a 12 bit monochrome CCD camera (QImaging QIClick-R-F-M-12). Borosilicate glass pipettes (Sutter Instrument BF100-58-10) with resistances ranging from 3–7 MΩ. were pulled using a laser micropipette puller (Sutter Instrument Model P-2000). For hippocampal neuron cultures, electrophysiological recordings from neurons were obtained in Tyrode's medium ([mM] 150 NaCl, 4 KCl, 2 $MgCl_2$, 2 $MgCl_2$, 10 D-glucose, 10 HEPES; 320 mOsm; pH adjusted to 7.35 with NaOH), AcOH Tyrode's medium ([mM] 125 NaCl, 25 AcOH, 4 KCl, 2 $MgCl_2$, 2 $MgCl_2$, 10 D-glucose, 10 HEPES; 320 mOsm; pH adjusted to 7.35 with NaOH) or L-lactate Tyrode's medium ([mM] 100 NaCl, 50 L-lactate, 4 KCl, 2 $MgCl_2$, 2 $MgCl_2$, 10 D-glucose, 10 HEPES; 320 mOsm; pH adjusted to 7.35 with NaOH), where indicated. The recording chamber was perfused at 0.5 ml min^{-1} and maintained at 29°C. Pipettes were filled using standard intracellular solution ([mM] 135 K-gluconate, 4 KCl, 2 NaCl, 10 HEPES, 4 EGTA, 4 MgATP, 0.3 NaGTP; 280 mOsm kg^{-1}; pH adjusted to 7.3 with KOH) or an intracellular solution allowing for EPSC and IPSC recording ([mM] 120 Cs-gluconate, 11 CsCl, 1 $MgCl_2$, 1 $CaCl_2$, 10 HEPES, 11 EGTA, 5 QX-314; 280 mOsm kg^{-1}; pH adjusted to 7.3 with CsOH). For acute brain slice experiments, whole-cell patch clamp recordings were obtained from layer 4 neurons of the barrel cortex, in regions showing robust axonal expression (mCherry fluorescence). During voltage clamp experiments neurons were clamped at either –70 mV or 0 mV to measure EPSCs or IPSCs, respectively. To calculate the paired-pulse ratio, pairs of electrical microstimulation pulses were delivered at 100 ms inter-pulse interval. To aid in visualization, Alexa Fluor 350 (Invitrogen, 100 μM) was included in some of the patch pipettes. Whole-cell voltage clamp recordings were performed using a MultiClamp 700B amplifier, filtered at 8 kHz and digitized at 20 kHz using a Digidata 1440A digitizer (Molecular Devices).

Two-photon Ca^{2+} and BCECF imaging

Imaging of the genetically encoded calcium sensor SyGCaMP6s was performed using a two-photon microscope (Ultima IV, Bruker) equipped with a 20x objective (NA 0.5). SyGCaMP6s was excited with a mode locked Ti:Sapphire laser tuned to 940 nm (Chameleon, Coherent) using a dwell time of 2.4 μs per pixel. Fluorescence was detected by a GaSP photomultiplier (Hamamatsu) after passing through a 525/50 nm filter. Images of 295 μm × 295 μm (1024 × 1024 pixels) area were recorded at 0.33 Hz to minimize

photobleaching. To record intracellular pH in cultured neurons, we used the pH-sensitive dye 2′,7′-Bis-(2-Carboxyethyl)-5-(and-6)-Carboxyfluorescein (BCECF). In these experiments, hippocampal neuron cultures expressing eArch3.0 or eNpHR3.0 were incubated for 10 min in BCECF-AM (TEFLABS) loading solution ([mM] 150 NaCl, 4 KCl, 2 $MgCl_2$, 2 $MgCl_2$, 10 D-glucose, 10 HEPES, 1×10^{-3} BCECF-AM; 320 mOsm; pH adjusted to 7.35 with NaOH). Fluorescence of BCECF was excited at the pH-sensitive two-photon wavelength 795 nm.

Stimulation and drug application

For activation of thalamocortical fibers, an extracellular stimulating electrode (concentric bipolar Pt/Ir electrode, 33 G; FHC) was placed in the external capsule in close proximity to visually identified mCherry-expressing fiber bundles. Fibers were activated by short, bipolar electrical pulses (400 μs, <100 μA). Opsins were activated using a 590 nm light emitting diode (LED; M590L2-C2; Thorlabs) delivered through the microscope illumination path which included a custom dichroic in order to reflect the 590 nm activation wavelength while collecting green fluorescence emission. Light power densities were calculated by measuring the light transmitted through the objective using a power meter (Thorlabs PM100A with S146C sensor) and dividing by the illumination area, calculated from the microscope objective field number and magnification25. TTX (1 μM; T-550, Alomone), D-AP5 (25 μM; ab120003; Abcam) and CNQX (10 μM; C-141, Alomone) were bath applied where indicated.

Data analysis and statistical methods

During whole-cell recordings, pClamp 10 software (Molecular Devices) was used for acquisition. Data was analyzed using custom scripts written in Matlab (Mathworks). EPSCs and IPSCs were automatically detected during periods in which cells were held at negative and positive membrane potentials, respectively. Holding current traces were filtered at 400 Hz using a 5th order lowpass Butterworth filter and deflections in the filtered trace were detected by threshold crossing of a 4 ms sliding window variance calculation. A suitable variance threshold was determined by recordings in the presence of synaptic blockers (25 μM D-AP5, 10 μM CNQX). To quantify postsynaptic current amplitudes evoked by electrical microstimulation, holding current traces were filtered with a Savitzky-Golay 11 point, second order, Welch window function filter and the maximal change in holding current within 5 ms (eEPSCs) and 10 ms (eIPSC) after electrical microstimulation was determined. For display purposes only, electrical microstimulation artifacts were manually removed. Fiji26 (based on ImageJ2; US National Institutes of Health) and Matlab were used for image analysis. Co-localization of SyGCaMP6s fluorescence with anti-Synapsin 1 staining was repeated 3 times and quantified using Manders split coefficients25 and Costes P-Value6. 87.7 % of the SyGCaMP6s signal above threshold significantly colocolized with 87.5% of the Synapsin 1 staining above threshold (Thresholded Manders M1 and M2: 0.877 and 0.875; Costes P-Value: 1.00).

For SyGCaMP6s and BCECF fluorescence analysis, images were smoothed by convolution with a Gaussian function (σ = 0.29 μm) and fluorescence background, measured from a manually defined region with no neurons, was subtracted to correct for bleed-through of

fluorescence and tissue autofluorescence excited by the opsin activation light (590 nm). Motion correction was performed using the image stabilizer ImageJ plugin (http://www.cs.cmu.edu/~kangli/code/Image_Stabilizer.html). Pixels above threshold, defined by Renyi's entropy method, were used for further analysis. Fluorescence traces are expressed as relative mean fluorescence change, $\Delta F/F = (F–F_0)/F_0$, where F_0 is the background-corrected minimal fluorescence during the baseline period. In case of Ca^{2+}-free recordings, F_0 is defined as the background-corrected minimal fluorescence after 2 mM Ca^{2+} reconstitution. In case of L-lactate recordings, F_0 is defined as the background-corrected minimal fluorescence before L-Lactate application. No temporal filtering was performed on the fluorescence transients for analysis. In imaging experiments, all numbers (n) refer to the number of imaged regions (each including neurites of multiple cells), while in electrophysiological recordings, n refers to the number of neurons. All values are indicated as mean ± s.e.m. Significance was determined at a significance level of 0.05 using paired two-tailed t tests in Fig. 2 (c,d,f,g), Fig. 3 (c,e), Supplementary Fig. 2 (c,d,g,h) and Supplementary Fig. 7d, One-Way ANOVA in Fig. 1 (e,h) with Bonferroni post-hoc tests, and Repeated Measures ANOVA with Bonferroni post-hoc tests for all other comparisons. Data shown in Fig. 1 (d,e,g,h) were log transformed before statistical comparison to compensate for unequal variance. A Huynh-Feldt correction was performed on data shown in Fig. 2 (e,h,j), Supplementary Fig. 2 (i), Supplementary Fig. 3c and Supplementary Fig. 4b to correct for violations of sphericity. No statistical tests were run to predetermine sample size, but sample sizes were similar to those commonly used in the field19,27. Blinding and randomization were not performed; however, automated analysis was used whenever possible. Supplementary Table 1 contains detailed descriptions of all of the statistical tests used in this study.

Supplementary Material

Refer to Web version on PubMed Central for supplementary material.

Acknowledgements

We thank M. Segal for helpful discussions and reagents. We thank Y. Ziv, L. Fenno, I. Lampl, R. Paz and the Yizhar lab members for comments on the manuscript. We acknowledge support (to O.Y.) from: the Human Frontier Science Program, the I-CORE program of the Planning and Budgeting Committee and the Israel Science Foundation (I-CORE grant no. 51/11, ISF grant no. 1351/12), a Marie Curie reintegration grant (CIG grant no. 321919), an ERC starting grant (no. 337637), the Adelis Foundation, the Lord Sieff of Brimpton Memorial Fund and the Candice Appleton Family Trust. O.Y is the incumbent of the Gertrude and Philip Nollman Career Development Chair.

References

1. Zhang F, et al. Nature. 2007; 446:633–639. [PubMed: 17410168]
2. Chuong AS, et al. Nat Neurosci. 2014; 17:1123–1129. [PubMed: 24997763]
3. Chow BY, et al. Nature. 2010; 463:98–102. [PubMed: 20054397]
4. Berndt A, Lee SY, Ramakrishnan C, Deisseroth K. Science. 2014; 344:420–424. [PubMed: 24763591]
5. Wietek J, et al. Science. 2014; 344:409–412. [PubMed: 24674867]
6. Govorunova EG, Sineshchekov OA, Janz R, Liu X, Spudich JL. Science. 2015; 349:647–650. [PubMed: 26113638]

7. Tye KM, et al. Nature. 2011; 471:358–362. [PubMed: 21389985]
8. Stuber GD, et al. Nature. 2011; 475:377–380. [PubMed: 21716290]
9. Spellman T, et al. Nature. 2015; 522:309–314. [PubMed: 26053122]
10. Gradinaru V, et al. Cell. 2010; 141:154–165. [PubMed: 20303157]
11. Fletcher TL, Cameron P, De Camilli P, Banker G. J Neurosci. 1991; 11:1617–1626. [PubMed: 1904480]
12. Fino E, Yuste R. Neuron. 2011; 69:1188–1203. [PubMed: 21435562]
13. Gabernet L, Jadhav SP, Feldman DE, Carandini M, Scanziani M. Neuron. 2005; 48:315–327. [PubMed: 16242411]
14. Chen YH, Wu ML, Fu WM. J Neurosci. 1998; 18:2982–2990. [PubMed: 9526015]
15. Tombaugh GC, Somjen GG. J Neurophysiol. 1997; 77:639–653. [PubMed: 9065837]
16. Turecek R, Trussell LO. Nature. 2001; 411:587–590. [PubMed: 11385573]
17. Pugh JR, Jahr CE. J Neurosci. 2011; 31:565–574. [PubMed: 21228165]
18. Price GD, Trussell LO. J Neurosci. 2006; 26:11432–11436. [PubMed: 17079672]
19. Raimondo JV, Kay L, Ellender TJ, Akerman CJ. Nat Neurosci. 2012; 15:1102–1104. [PubMed: 22729174]
20. Cosentino C, et al. Science. 2015; 348:707–710. [PubMed: 25954011]
21. Chen TW, et al. Nature. 2013; 499:295–300. [PubMed: 23868258]
22. Dreosti E, Odermatt B, Dorostkar MM, Lagnado L. Nat Methods. 2009; 6:883–889. [PubMed: 19898484]
23. Fenno LE, et al. Nat Methods. 2014; 11:763–772. [PubMed: 24908100]
24. Grimm D, Kay MA, Kleinschmidt JA. Mol Ther. 2003; 7:839–850. [PubMed: 12788658]
25. Grunwald D, Shenoy SM, Burke S, Singer RH. Nat Protoc. 2008; 3:1809–1814. [PubMed: 18974739]
26. Schindelin J, et al. Nat Methods. 2012; 9:676–682. [PubMed: 22743772]
27. Mattis J, et al. Nat Methods. 2012; 9:159–172. [PubMed: 22179551]

Europe PMC Funders Author Manuscripts

Europe PMC Funders Author Manuscripts

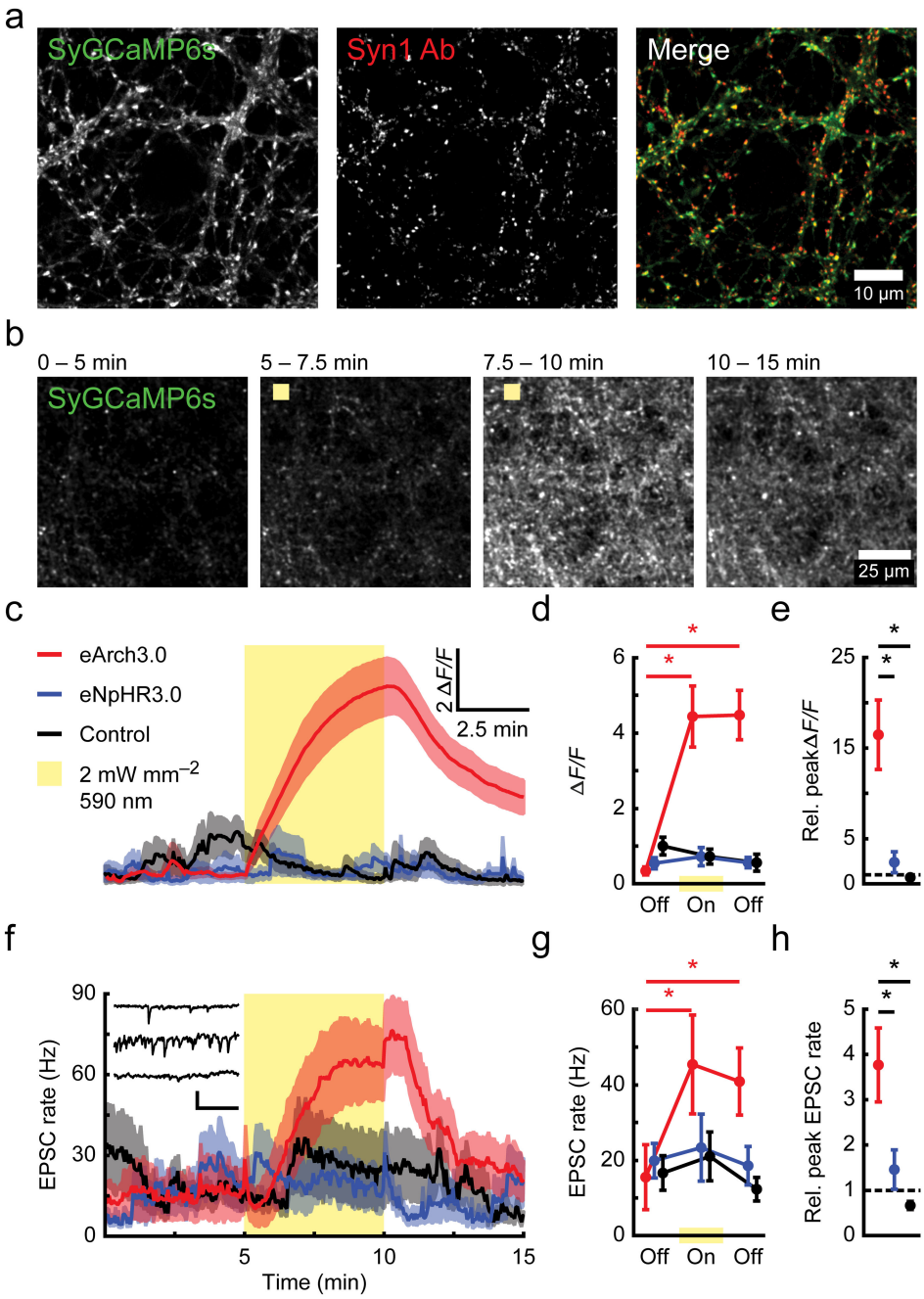

Figure 1. Sustained activation of eArch3.0 increases presynaptic Ca^{2+} and neurotransmitter release.

(a) Evaluation of SyGCaMP6s targeting to the presynaptic terminal. Left: cultured neurons expressing SyGCaMP6s; center: anti-Synapsin I labeling; right: merge. **(b)** Representative time-averaged images acquired during the indicated time periods from a hippocampal neuron culture co-expressing SyGCaMP6s and eArch3.0. **(c–d)** Relative fluorecence change from baseline (*ΔF/F*) of spontaneously active neuronal cultures expressing SyGCaMP6s. **(d)** Average *ΔF/F* during baseline, light (590 nm, 2 mW mm^{-2}) and post-light periods depicted

Europe PMC Funders Author Manuscripts

in **c.** Neurons co-expressing eArch3.0 ($n = 12$) showed increased SyGCaMP6s signal compared with neurons expressing eNpHR3.0 ($n = 12$) and controls ($n = 8$). **(e)** Peak SyGCaMP6s fluorescence during 590 nm illumination relative to peak SyGCaMP6s fluorescence during baseline activity of neurons expressing SyGCaMP6s (control) or co-expressing SyGCaMP6s with eArch3.0 or eNpHR3.0. Dotted line indicates zero. **(f)** Average EPSC rates recorded in neuronal cultures expressing the indicated constructs. Inset depicts representative voltage clamp recording traces of an eArch3.0 expressing culture before (top), during (middle) and after (bottom) 590 nm illumination (scale bar, 30 pA, 150 ms). **(g)** Average EPSC rates during baseline, light and post-light periods, as depicted in **f** (control, $n = 11$; eNpHR3.0, $n = 12$; eArch3.0, $n = 12$). **(h)** Peak EPSC rates during illumination relative to peak EPSC rates during baseline. Dotted line indicates one. Error bars and shaded regions indicate s.e.m. (* $P < 0.01$; see Supplementary Table 1 for statistics).

Europe PMC Funders Author Manuscripts

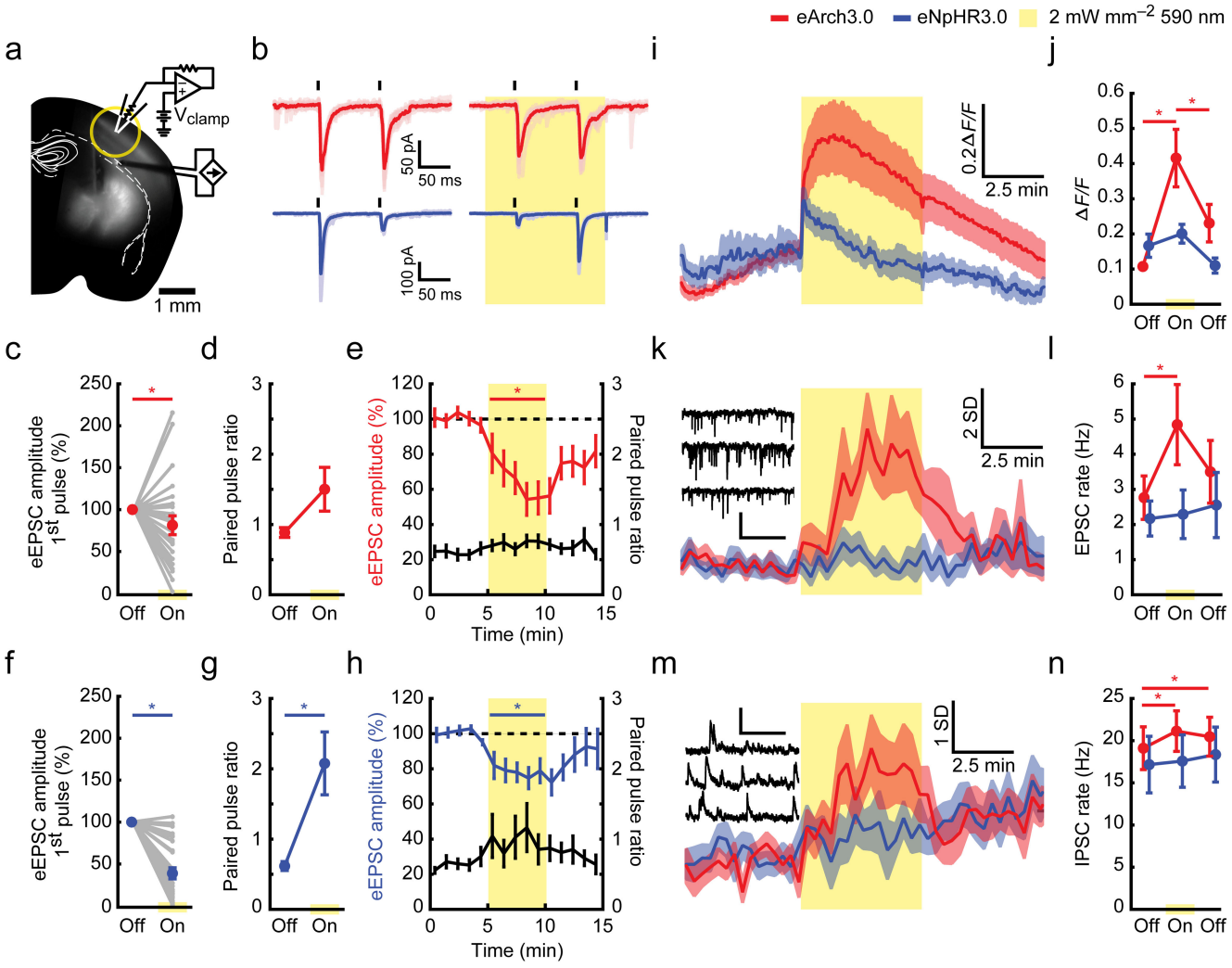

Figure 2. Effects of eArch3.0 and eNpHR3.0 on evoked and spontaneous release in thalamocortical terminals.

Characterization of presynaptic terminal inhibition in acute brain slices using the microbioal ion transporters eArch3.0 and eNpHR3.0. **(a)** Schematic illustration of the experimental setup. The bipolar stimulation electrode was placed in the thalamocortical fiber tract, while whole-cell voltage clamp recordings were performed in layer 4 of barrel cortex. Yellow circle indicates area of light application for opsin acivation. **(b)** Example traces of EPSCs evoked by electrical microstimulation (eEPSCs) with and without light application to the presynaptic terminals. Individual traces are overlaid with their mean. Black ticks indicate time of electrical stimulation. **(c,d,f,g)** Quantification of eEPSCs before and during brief light application (200 ms, 590 nm, 2 mW mm^{-2}; **(c)** $n = 24$, $P = 0.019$. **(d)** $n = 24$, $P = 0.075$. **(f)** $n = 28$, $P = 1.03\times10^{-4}$ **(g)** $n = 28$, $P = 3.14\times10^{-3}$). **(e,h)** eEPSC amplitude relative to baseline and paired-pulse ratio during 5 min constant illumination. **((e)** eEPSC amplitude: $n = 10$; Paired pulse ratio: $n = 9$. **(h)** eEPSC amplitude: $n = 14$. Paired pulse ratio: $n = 14$) **(i)** SyGCaMP6s imaging of presynaptic boutons during the same light application protocol. **(j)** Quantification of average fluorescence during baseline, light and post-light periods shown in

i. (eArch3.0: $n = 9$; eNpHR3.0: $n = 6$). **(k,m)** Effect of constant illumination on spontaneous EPSC **(k)** and IPSC **(m)** rates (z-scores). Insets depict sample eArch3.0 traces from baseline (top), light (middle) and post-light (bottom) periods (scale bars, 40 pA, 200 ms). **(l,n)** Quantification of EPSC and IPSC rates from **k** and **m. ((l)** eArch3.0: $n = 13$. eNpHR3.0: $n = 10$; **(n)** eArch3.0: $n = 13$; eNpHR3.0: $n = 10$). Error bars and shading indicate s.e.m. (* $P < 0.05$; see Supplementary Table 1 for statistics).

Europe PMC Funders Author Manuscripts

Europe PMC Funders Author Manuscripts

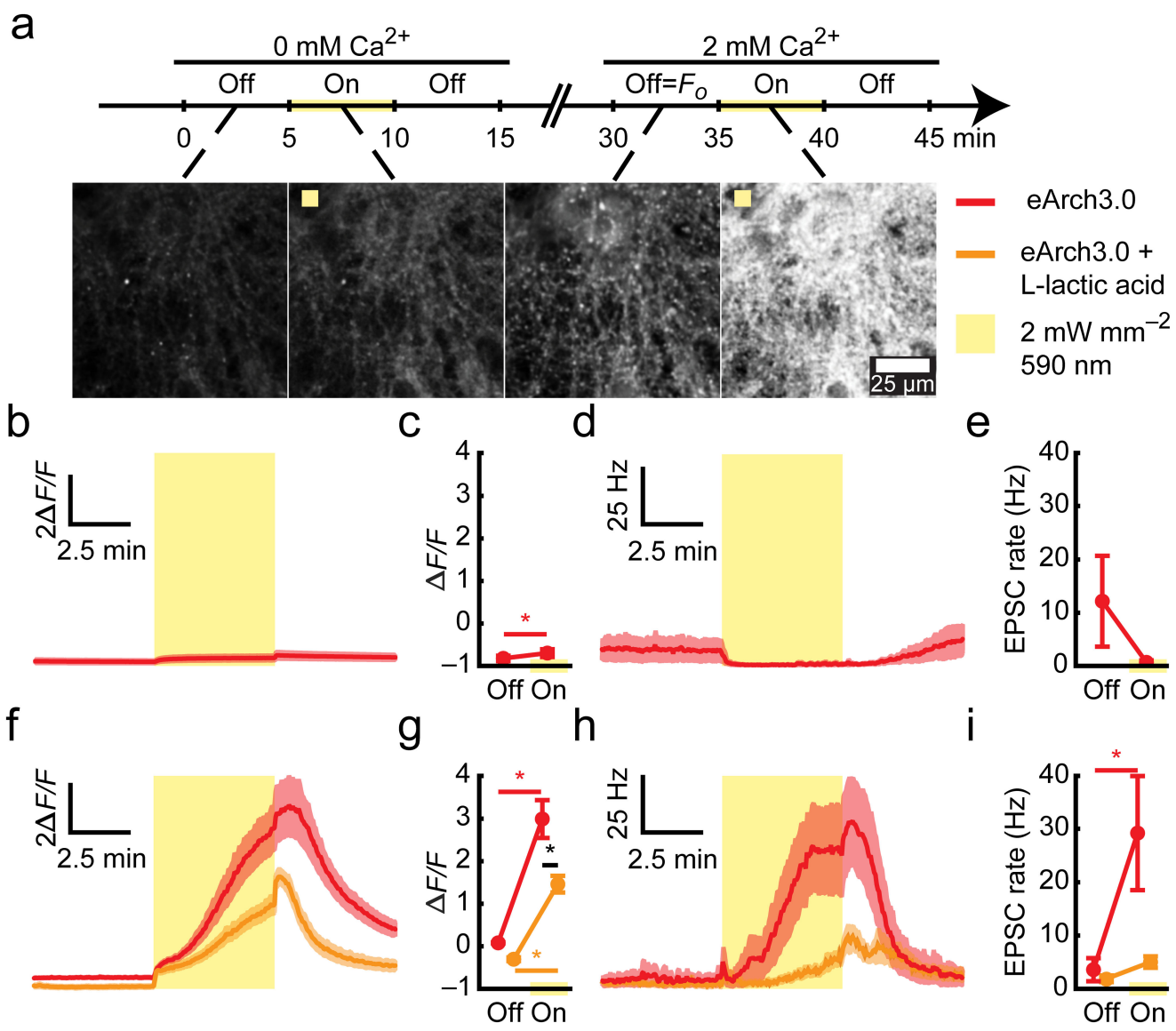

Figure 3. eArch3.0 activation triggers pH-dependent, TTX-insensitive calcium influx.

(a) Experimental time course: neurons expressing eArch3.0 and SyGCaMP6s were recorded in Ca^{2+}-free medium, followed by reintroduction of Ca^{2+} into the extracellular medium. Representative images depict average fluorescence during a 5 min baseline period followed by 5 min of 590 nm illumination. *AF/F* was calculated based on baseline fluorescence in 2 mM Ca^{2+}. **(b)** Time course of *ΔF/F* in Ca^{2+}-free medium. **(c)** Quantification of average *ΔF/F* during basline and light-on periods shown in **b** ($n = 10$, $P = 6.21\times10^{-3}$). **(d)** Time course of EPSC rates recorded in Ca^{2+}-free medium. **(e)** Quantification of average EPSC rates during baseline and light-on periods ($n = 5$, $P = 0.24$). **(f)** Time course of *ΔF/F* in neurons recorded in TTX (1 µM, red, $n = 10$) or in TTX and L-lactate (50 mM, pH = 7.3; orange, $n = 8$). *ΔF/F* was calculated based on baseline fluorescence in L-lactate free medium **(g)** Average *ΔF/F* during baseline and light-on periods shown in **f. (h)** Time course of EPSC rates recorded in TTX (red, $n = 9$) or in TTX and L-lactate (orange, $n = 9$). **(i)** Quantification of average

EPSC rates during baseline and light-on periods from **h.** Error bars and shaded regions indicate s.e.m. (* $P < 0.05$; see Supplementary Table 1 for statistics).

Europe PMC Funders Author Manuscripts